Materials Letters 187 (2017) 114–117

Contents lists available at ScienceDirect

Materials Letters

journal homepage: www.elsevier.com/locate/matlet

Facile synthesis of cubic-phase lithium tungsten oxide and its application in lithium storage

Yang Chen[a], Chunyang Song[a], Zhangfeng Li[b], Xiaoli Cui[a,*], Zhiyu Jiang[c]

[a] Department of Materials Science, Fudan University, Shanghai 200433, P. R. China
[b] Shanghai Institute of Space Power Sources, Shanghai 200245, P. R. China
[c] Department of Chemistry, Fudan University, Shanghai 200433, P. R. China

ARTICLE INFO

Keywords:
Energy storage and conversion
Functional
Lithium-ion batteries
Anode
Lithium tungsten oxide

ABSTRACT

A novel cubic-phase lithium tungsten oxide ($Li_6W_2O_9$) is synthesized via a citric acid assisted liquid-phase reaction at 80 °C followed by post-annealing, and the lithium storage is firstly demonstrated. The carbon-coated $Li_6W_2O_9$ is obtained after annealing at 500 °C under N_2 flow. The capacity of 255 mAh g^{-1} after 100 cycles at 50 mA g^{-1} is observed for the samples. The enhanced electrochemical performance is attributed to the presence of surface 2 nm carbon layer, which is confirmed by TEM measurement. The carbon coating has efficiently improved electrical conductivity and concurrently inhibited volume variation. The carbon-coated $Li_6W_2O_9$ could be a promising anode candidate for lithium-ion batteries.

1. Introduction

Currently, great progress has been made in transition metal oxides as competitive anode candidates for lithium-ion batteries (LIBs) owing to their high energy capability, low cost and natural abundance [1–3]. Tungsten-based oxides including tungsten trioxide and binary compounds, such as MWO_x (M=Mn, Co, Ni, Cu, Bi, Cd, Fe, Zn, etc.), can deliver high capacities due to the conversion mechanism with various oxidation states of W ranging from +6 to 0 reacting with large quantities of lithium ions [4–10].

Lithium tungsten oxides have been fabricated and employed as electrode supplemental materials [11,12]. For instance, a tetragonal Li_2WO_4-modified $LiCoO_2$ electrode was prepared by Hayashi's group through pulsed laser deposition [11]. The surface randomly oriented Li_2WO_4 decreased the charge transfer resistance between solid electrode and electrolyte. To the best of our knowledge, lithium tungsten oxides have not been investigated as anode materials for LIBs so far. We are highly interested in their lithium storage properties due to their high theoretical capacity. It is assumed to be 581–652 mAh g^{-1} with various stoichiometric ratio of Li and W (Tab. S1 in Supporting Information), which is much higher than that of commercially widely used graphite and $Li_4Ti_5O_{12}$ [13].

In this work, we proposed a facile citric acid-assisted synthesis route to fabricate a novel cubic-phase lithium tungsten oxide ($Li_6W_2O_9$) in the first time. Citric acid here is utilized as both assistant agent and carbon source. Lithium storage performance of the as-prepared samples was investigated, and good cycling stability and rate capability were demonstrated accordingly.

2. Experimental

Fig. 1 illustrates the synthesis procedure. Briefly, 1.11 g lithium carbonate (Li_2CO_3), 2.32 g tungsten trioxide (WO_3), and 0.32 g citric acid monohydrate ($C_6H_8O_7{\cdot}H_2O$) were added into 50 mL deionized water. The solution was evaporated by immersing the beaker in a water bath kept at 80 °C with constantly magnetic stirring to form a white xerogel, which was then dried at 80 °C under vacuum overnight. Then, the white intermediates were annealed in air and N_2 at 500 °C for 3 h to obtain pure $Li_6W_2O_9$ and carbon-coated $Li_6W_2O_9$ (denoted by $Li_6W_2O_9$/C), respectively.

The samples were characterized by X-ray diffraction (XRD), scanning electron microscope (SEM) and transmission electron microscopy (TEM). The lithium storage performance was evaluated by CR2016 coin-type cells using lithium foil as counter electrode. The electrode fabrication and cell assembly followed a similar process described in our previous work [14], and detailed characterization and electrochemical measurements can be found in Supporting Information.

3. Results and discussion

Fig. 2A shows XRD patterns of $Li_6W_2O_9$ xerogel intermediate (a), pure $Li_6W_2O_9$ (b) and $Li_6W_2O_9$/C (c). All observed reflection patterns

* Corresponding author.
E-mail address: xiaolicui@fudan.edu.cn (X. Cui).

http://dx.doi.org/10.1016/j.matlet.2016.10.086
Received 5 August 2016; Received in revised form 28 September 2016; Accepted 21 October 2016
Available online 22 October 2016
0167-577X/

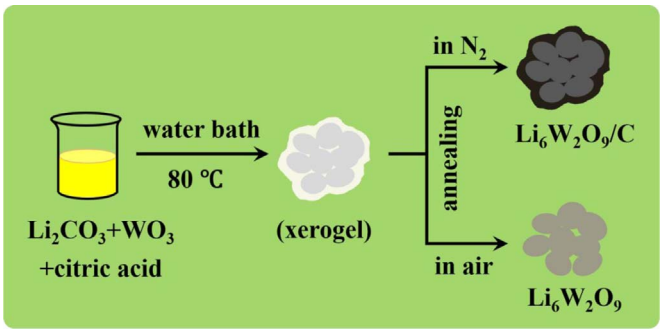

Fig. 1. Schematic illustration of the synthesis of $Li_6W_2O_9$/C and pure $Li_6W_2O_9$.

of three samples can match exactly with cubic-phase $Li_6W_2O_9$ referring to the standard spectrum (JCPDS 25–0503). This crystal structure adopts space group Pm-3 m (221), where a=b=c and α=β=γ=90° [15]. Besides, the perfect $Li_6W_2O_9$ crystal structure is directly formed in the liquid-phase reaction process at 80 °C, showing an attractive energy-saving advantage compared with solid-phase fabrication [16]. Meanwhile, no peaks belonging to carbon species can be distinguished in the pattern of the $Li_6W_2O_9$/C sample, which may be due to the nature of amorphous carbon or relative low carbon content below the level of detection. And it is reasonable that the presence of carbon does not have any effect on the crystal structure of $Li_6W_2O_9$.

Fig. 2B~D depict SEM images of the as-prepared samples. As shown in Fig. 2B, C, the carbon-coated and pure $Li_6W_2O_9$ samples are composed of spherical-like bulk particles in the average size range of 1–3 μm with irregular surface. For the $Li_6W_2O_9$ xerogel intermediate (Fig. 2D), the particles are buried in the organic substance forming an interconnected cover layer. In addition, it can be identified from inserted digital photographs that the color of pure $Li_6W_2O_9$ is beige [16], while the $Li_6W_2O_9$/C sample is black on account of carbon coating and the xerogel intermediate is white due to the presence of surface organic layer.

The microstructure of the $Li_6W_2O_9$/C sample was further explored by TEM. As shown in Fig. 3A, a coating layer can be observed on the surface of $Li_6W_2O_9$. In the HRTEM image (Fig. 3B), highly ordered lattice fringes with a space of 0.21 nm can be distinguished, which are in good correspondence to the characteristic (400) crystalline plane of cubic phase $Li_6W_2O_9$ [15]. The thickness of surface carbon layer is approximate 2 nm. And it can be seen from supplementary Fig. S1 that the total carbon content in $Li_6W_2O_9$/C is approximate 2.5%. The selected area electron diffraction (SAED) patterns display a series of diffraction ring relating to various lattice plane. Furthermore, it can be clearly observed from the energy dispersed spectrum (EDS) mapping (Fig. 3D) that the dominant distribution of carbon element is around the edges of particles, indicating the above-mentioned structure with surface carbon coating.

The potential application on lithium storage was evaluated in lithium half-cells using $Li_6W_2O_9$/C and pure $Li_6W_2O_9$ as anode active materials. Fig. 4A displays the first three cycles of cyclic voltammetry (CV) curves for the $Li_6W_2O_9$/C sample. A prominent reduction peak located at 0.1 V in the initial cathodic sweep is associated with the conversion of $Li_6W_2O_9$ reacting with lithium ions, which accords with the following mechanism (Eq. (1)). And two anodic peaks at 0.4 V and 1.0 V is attributed to the stepwise delithiation process as demonstrated in the Eq. (2), which delivers subsequent reversible capacities [17]. Ex-situ XRD analysis were carried out to further clarify the electrochemical process for the first discharge–charge cycle, and the patterns are shown in supplementary Fig. S2 coupled with corresponding detail discussion.

$$Li_6W_2O_9 + 12\,Li^+ + 12\,e^- \rightarrow 2\,W + 9\,Li_2O \quad (1)$$

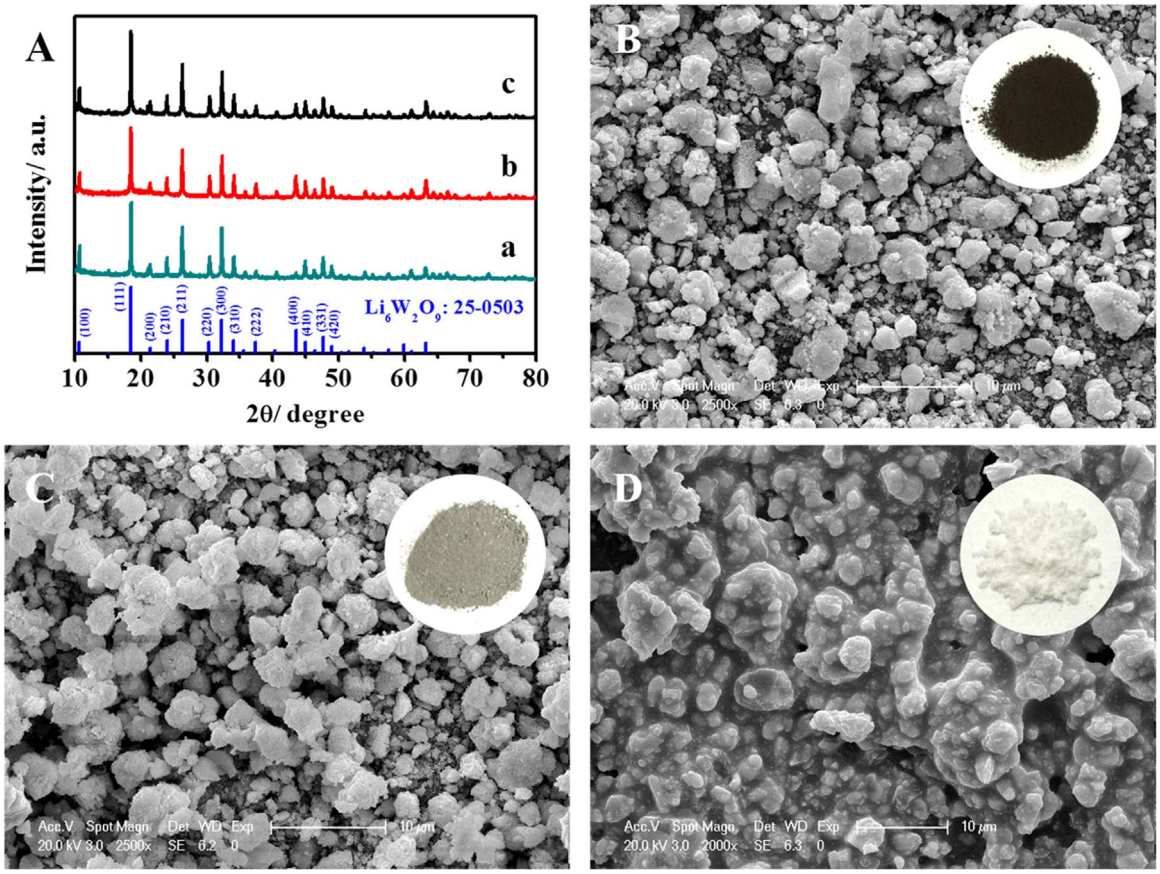

Fig. 2. (A) XRD patterns of $Li_6W_2O_9$ xerogel intermediate (a), pure $Li_6W_2O_9$ (b) and $Li_6W_2O_9$/C (c). SEM images of (B) $Li_6W_2O_9$/C, (C) pure $Li_6W_2O_9$ and (D) $Li_6W_2O_9$ xerogel intermediate; respective digital photographs as inserts.